



## EDGE ARTICLE

Cite this: *Chem. Sci.*, 2024, 15, 4171

All publication charges for this article have been paid for by the Royal Society of Chemistry

# $\epsilon$ -Polylysine organic ultra-long room-temperature phosphorescent materials based on phosphorescent molecule doping†

Jiaying Cui,<sup>a</sup> Syed Husnain Ali,<sup>a</sup> Zhuoyao Shen,<sup>a</sup> Wensheng Xu,<sup>a</sup> Jiayi Liu,<sup>a</sup> Pengxiang Li,<sup>a</sup> Yang Li,<sup>a</sup> \*<sup>ac</sup> Ligong Chen <sup>abc</sup> and Bowei Wang \*<sup>abc</sup>

Achieving long-lived room-temperature phosphorescence from pure organic amorphous polymers is attractive, and afterglow materials with colour-tunable and multiple-stimuli-responsive afterglow are particularly important, but only few materials with these characteristics have been reported so far. Herein, a facile and general method is reported to construct a series of  $\epsilon$ -polylysine ( $\epsilon$ -PL)-based afterglow materials with tunable colour (from blue to red) and long life. By doping guest molecules into  $\epsilon$ -PL to obtain composite materials, the polymer matrix provides a rigid environment for luminescent groups, resulting in amorphous polymers with different RTPs. In this system, the materials even have impressive humidity-stimulated responses, and the phosphorescence emission exhibits excitation-dependent and time-dependent properties. The humidity-responsive afterglow is caused by the destruction of hydrogen bonds and quenching of triplet excitons. The time-dependent afterglow should stem from the formation of diversified RTP emissive species with comparable but different lifetimes. 9,10-diaminophene has Ex-De properties in the film doping state. With the change of excitation wavelength (254 nm to 365 nm), the emission wavelength shifts from 461 nm to 530 nm, accompanied by the change of emission colour from blue to green. In addition, the phosphorescence life of the film is the longest, up to 2504.7 ms, and the afterglow lasts up to 15 s, which is conducive to its applications in anti-counterfeiting and information encryption.

Received 23rd November 2023

Accepted 2nd February 2024

DOI: 10.1039/d3sc06271f

rsc.li/chemical-science

## Introduction

In recent years, afterglow materials have attracted great attention because of their unique properties.<sup>1,2</sup> Currently, a large number of inorganic afterglow materials have been developed; however, rare earth materials used in the preparation of inorganic afterglow materials are expensive and synthesis processes are complicated, limiting their further development. Compared to inorganic counterparts, organic room-temperature phosphorescent (RTP) materials have the advantages of low cost, rich sources, easy synthesis and adjustable structures.<sup>3</sup> They have attractive application prospects in many high-tech fields, such as bioimaging, optical recording, information storage, encryption and anti-counterfeiting systems.<sup>4–8</sup> In general, the promotion of organic RTP follows two principles: one is to promote intersystem crossing (ISC) and the other is to inhibit non-

radiative transitions and slow down the quenching of triplet excitons.<sup>3,9</sup> Many strategies spanning from  $\pi$ - $\pi$  stacking interactions<sup>10,11</sup> to host-guest approaches,<sup>12,13</sup> crystallization<sup>14,15</sup> and cocrystallization,<sup>16,17</sup> carbon dots (CDs),<sup>18–21</sup> heavy atoms effect<sup>22,23</sup> and doping in a polymer matrix<sup>24–26</sup> have been developed to realize the RTP of organic materials. Among them, polymer-based phosphorescent materials have been receiving increasing attention because they not only possess fantastic properties, such as good flexibility, high transparency, and high thermal stability but also serve as rigid matrices to suppress the nonradiative decay process, further promoting phosphorescence emission at room temperature.<sup>27–30</sup> For example, Wu *et al.*<sup>31</sup> successfully prepared a series of polymer-based RTP films, showing good film-forming, elasticity, flexibility and RTP properties.

Nevertheless, achieving a wide-range and colour-adjustable afterglow emission remains a tough challenge.<sup>32</sup> Lei *et al.*<sup>33</sup> developed a series of novel host-guest organic phosphors allowing dynamic colour tuning from cyan to orange red. However, the narrow emission wavelength coverage (502–608 nm) and limited tunable colours greatly limit their application. Therefore, further development of a versatile platform to realize RTP emissions from blue to red is highly desired.<sup>3</sup> In addition, most materials reported so far do not achieve multiple stimulus

<sup>a</sup>School of Chemical Engineering and Technology, Tianjin University, Tianjin, 300350, P. R. China. E-mail: bwwang@tju.edu.cn; liyang777@tju.edu.cn

<sup>b</sup>Zhejiang Institute of Tianjin University, Shaoxing, 312300, P.R. China

<sup>c</sup>Tianjin Engineering Research Center of Functional Fine Chemicals, Tianjin, 300350, P.R. China

† Electronic supplementary information (ESI) available. See DOI: <https://doi.org/10.1039/d3sc06271f>



responses,<sup>34</sup> and only a few materials show time-dependent<sup>15</sup> and excitation-dependent<sup>35</sup> emissions. For example, Su *et al.*<sup>36</sup> developed a suitable strategy to achieve excitation-dependent phosphorescence emission under ambient conditions using metal-free amorphous organic materials to increase ISC pathways by the formation of controlled aggregation. Although some RTP materials with specific properties have been successfully reported, current organic RTP materials present short phosphorescence lifetimes of only hundreds of milliseconds and poor stability; work on long-lifetime phosphorescence emission with afterglow time > 15 s under environmental conditions is rarely reported. This cannot be ignored, as it greatly limits their potential applications.<sup>10,37–39</sup> In this context, amorphous organic polymers with long-lived RTP are more competitive in materials science. Non-covalent interactions between polymers and guest molecules play a vital role in limiting the movement of the guest molecules and reducing the loss of non-radiative transitions. They also shield the quenching of triplet excitons by water and oxygen, which is conducive to the realization of ultralong and bright RTP emissions.

Therefore, developing a colour-tunable, long-lived polymer-based RTP material with multiple responses to external stimuli remains highly challenging. Herein, we reported an  $\epsilon$ -polylysine ( $\epsilon$ -PL)-based RTP material with excellent RTP properties by the simple doping of phosphorescent guest molecules into it (Fig. 1a). By doping a reasonably selected heterocyclic polynuclear aromatic compound as a guest molecule into the  $\epsilon$ -PL matrix, full-spectrum afterglow emission from blue to red was achieved (Fig. 1b). On the one hand, electrostatic interactions and abundant hydrogen bonds between  $\epsilon$ -PL and the guest molecules could provide a rigid environment, inhibit non-radiative transitions, and promote phosphorescence emission. On the other hand, doped guest molecules containing N, O and S elements can promote an n- $\pi$  transition,<sup>40</sup> increasing spin-

orbit coupling (SOC) and promoting intersystem crossing (ISC). Gratifyingly, Daphe@ $\epsilon$ -PL films exhibited excitation-dependent properties with phosphorescence lifetime of up to 2504.7 ms (Fig. 1c), while ANS@ $\epsilon$ -PL films exhibited time-dependent afterglow (Fig. 1d). Based on their excellent film-forming capabilities, these polymers are promising for advanced technical applications like anti-counterfeiting and information.

## Results and discussion

A series of heterocyclic aromatic compounds were selected and doped into the  $\epsilon$ -PL matrix at a mass ratio of 1 : 100 at 50 °C. The SEM images of the obtained five kinds of  $\epsilon$ -PL-based RTP films (Daphe@ $\epsilon$ -PL, NDA@ $\epsilon$ -PL, ANA@ $\epsilon$ -PL, ANS@ $\epsilon$ -PL, and Apyr@ $\epsilon$ -PL) indicated that they were successfully doped with the guest molecules (ESI Fig. S1†). Under ultraviolet light illumination, these materials exhibit blue or cyan photoluminescent emission (Fig. 2a). After the UV light was turned off, a blue to red afterglow lasting up to 15 seconds was observed (Fig. 2a; ESI S2 and Videos S1–S5†). To study their photophysical properties in detail, their excitation spectra (ESI Fig. S3†), photoluminescence spectra (ESI Fig. S4†) and delayed phosphorescence spectra (ESI Fig. S5†) were tested (Fig. 2b). Compared to steady-state phosphorescence spectra, the peaks of their delayed phosphorescence spectra were generally redshifted (Fig. 2b), which matched their S<sub>1</sub> and T<sub>1</sub> energy levels. These results fully manifested that their delayed PL spectra exhibit phosphorescence emission. It can be clearly seen from the spectral diagram that the phosphorescence wavelength of the five  $\epsilon$ -PL-based RTP films ranges from 508 nm to 693 nm under the excitation of the 365 nm UV light, and multi-colour afterglow can be observed. The Commission Internationale de l'Éclairage (CIE) coordinates of the afterglows are shown in Fig. 2c, and the coordinates of the Daphe, NDA, ANA, ANS, Apyr-doped  $\epsilon$ -PL systems are located at (0.27, 0.35), (0.33, 0.47), (0.43, 0.51), (0.51, 0.46), and (0.42, 0.34), respectively. These coordinates correspond to a colour change from blue to red, which was consistent with the colour change observed by the naked eye. Encouragingly, the quantum yields of these  $\epsilon$ -PL-based RTP films were as high as 18.84% (ESI, Table S1†). Surprisingly, the longest phosphorescence lifetime was up to 2505 ms (Fig. 2d and ESI S6†). To further exclude the polymer matrix as the phosphorescence source, the spectrum of  $\epsilon$ -PL was collected. It was found that  $\epsilon$ -PL presented phosphorescence emission at 430 nm and 516 nm (ESI Fig. S7†), which was quite close to the used phosphorescent guests, but its lifetime was only a few milliseconds (ESI Fig. S8†), which was insignificant compared with the phosphorescence lifetimes of the doped guest molecules and would not affect the RTP performance of the films. Therefore, the doped guest molecules remained the main sources of phosphorescence. Furthermore, the phosphorescence spectra of the five guest molecules were collected at 77 K (ESI Fig. S9†). Compared with the spectra of the five  $\epsilon$ -PL-based RTP films, it could be concluded that the afterglows of different colours came from the guest molecules.

To explore the effect of guest molecule doping dose on the phosphorescence lifetime of the RTP films, Daphe@ $\epsilon$ -PL films with doping content ranging from 0.1% to 1.5% (in mass ratio) were prepared. As shown in Fig. 2e (and ESI Fig. S10†), with the

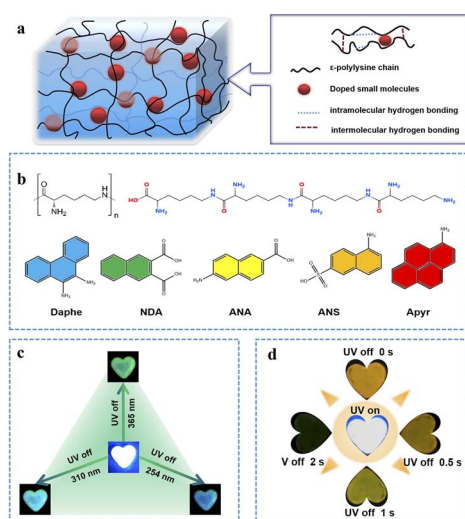


Fig. 1 (a) Schematic diagram of matrix-doped guest molecules. (b) Chemical structure of  $\epsilon$ -polylysine and five guest phosphorescent molecules. (c) Schematic diagram of an excitation-dependent RTP system. (d) Schematic diagram of a time-dependent RTP system.

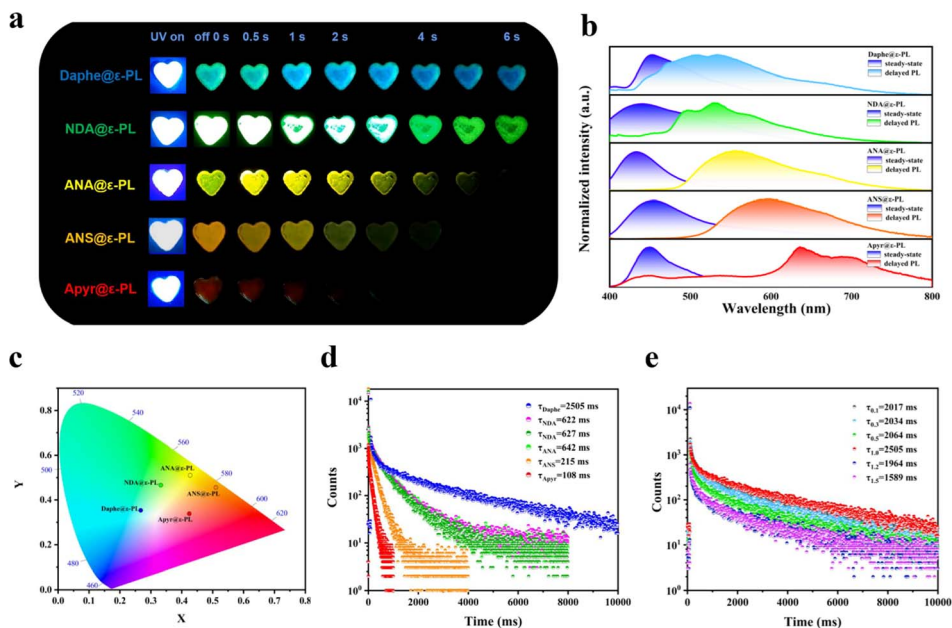


Fig. 2 (a) Photographs of Daphe@ $\epsilon$ -PL, NDA@ $\epsilon$ -PL, ANA@ $\epsilon$ -PL, ANS@ $\epsilon$ -PL, and Apyr@ $\epsilon$ -PL taken under 365 nm UV light or after ceasing the irradiation. (b) Steady-state and delayed ( $t_d = 0.1$  ms) PL spectra of the five  $\epsilon$ -PL-based RTP films. (c) The CIE coordinate diagram of the colours of the phosphorescence emitted by the five  $\epsilon$ -PL-based RTP films. (d) Time-resolved emission decay curves of the five  $\epsilon$ -PL-based RTP films at different wavelengths. (e) Time-resolved emission decay curves of Daphe@ $\epsilon$ -PL films with different doping contents.

increase of the doping amount, the phosphorescence lifetimes increased first and then decreased. The phosphorescence lifetime at 471 nm reached a maximum of 2505 ms when the doping content was 1.0%. Therefore, the optimal guest molecule doping content in the  $\epsilon$ -PL-based RTP films was determined to be 1.0%. Subsequently, the optimal content of other guest molecules was also determined to be 1.0%.

Notably, the phosphorescence of Daphe@ $\epsilon$ -PL showed obvious excitation dependence (Fig. 3a). To further explore the mechanism of phosphorescence Ex-De properties, the delayed phosphorescence spectra (Fig. 3b), the photoluminescence spectra (Fig. 3e) and lifetime decay curves (Fig. 3d) of Daphe@ $\epsilon$ -PL under different UV excitation wavelengths were collected. The wavelength of the emission peak greatly varied under

different excitation wavelengths. Under the excitation of 254 nm UV light, the strongest emission peak in the delayed phosphorescence spectrum was located at 461 nm, the CIE chromaticity coordinate (Fig. 3c) was (0.23, 0.30), and the colour was blue, consistent with the observed colour. Upon the excitation of 310 nm UV light, the peak at 500 nm was significantly enhanced, and the CIE coordinate was (0.27, 0.35). At the same time, under the irradiation of this excitation light, the longest life of the RTP films reached 2505 ms (Fig. 3d and ESI Table S2<sup>†</sup>). When the excitation wavelength was increased to 365 nm, the emission spectrum redshifted to 530 nm, and the corresponding CIE coordinate became (0.31, 0.42). With the increase of the excitation wavelength, the intensity of the long wavelength peaks increased, while that of short wavelength peaks decreased. Such alteration of the excitation wavelength (from 254 to 365 nm) resulted in a significant difference in the spectra and a dramatic decrease in the lifetime, indicating that Daphe@ $\epsilon$ -PL is excitation-dependent. Because Daphe has a large  $\pi$ -conjugated structure, it is very easy to form aggregates through  $\pi$ - $\pi$  packing, and the formation of aggregates would cause exciton orbitals to overlap, resulting in energy level splitting. Coupled splitting of energy levels will produce more ISC channels and increase  $k_{isc}$ , thus promoting phosphorescence emission. To deeply understand the mechanism of the excitation-dependent luminescent behavior of Daphe@ $\epsilon$ -PL films, we controlled the doping contents of Daphe and measured the corresponding emission spectra (ESI, Fig. S11<sup>†</sup>). Taking Daphe@ $\epsilon$ -PL films excited at 310 nm UV light as an example, with the increase of Daphe doping content, the fluorescence peaks basically remained the same. The phosphorescence of Daphe@ $\epsilon$ -PL films showed three peaks at 461, 500 and

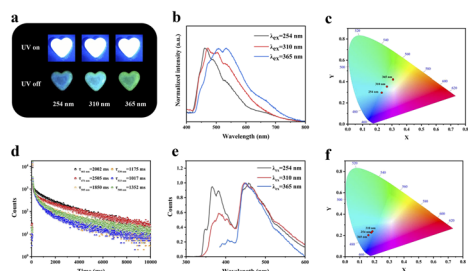


Fig. 3 (a) Photographs of Daphe@ $\epsilon$ -PL films taken under 254, 310, and 365 nm UV light or after ceasing the irradiation. (b) Delayed emission spectra. (c) CIE coordinate diagrams of Daphe@ $\epsilon$ -PL with different  $\lambda_{ex}$ s corresponding to delayed emission spectra. (d) Time-resolved emission attenuation curves of Daphe@ $\epsilon$ -PL films at different wavelengths taken under different UV light. (e) Photoluminescence spectra. (f) CIE coordinate diagrams corresponding to photoluminescence spectra.

530 nm. As the doping content of Daphe increased, the intensity of peaks at 530 nm significantly increased, whereas peaks at 461 nm gradually decreased, suggesting that more and more excitation energy is flowing into the low-energy emission pathway.<sup>41</sup> In addition, owing to the charge transfer caused by  $\pi$ - $\pi$  packing interaction, the energy level of the aggregate decreased, hence the delayed phosphorescence spectrum of Daphe@ $\epsilon$ -PL showed a redshift. The phosphorescence spectrum of Daphe@ $\epsilon$ -PL was excitation-dependent because the relative intensity of phosphorescence changes under the excitation of different wavelength UV light at different luminous centers. Meanwhile, this phenomenon can also be observed in concentrated solutions with distinct  $\pi$ - $\pi$  stackings (ESI Fig. S12<sup>†</sup>).

It was also noted that ANS@ $\epsilon$ -PL films exhibited time-dependent phosphorescence (ESI Fig. S13<sup>†</sup>). The colour of the afterglow changed from orange to yellow and finally to green. To study the photophysical properties of the time-dependent afterglow in detail, delayed phosphorescence spectra (Fig. 4a) and time-resolved decay curves (Fig. 4c) were characterized. As shown in Fig. 4a, as the delay time extended, the peak wavelength of its spectrum also presented a blueshift, resulting in the change of the afterglow colours and indicating the presence of multiple emission centers, which was attributed to the presence of monomers and aggregates of ANS.<sup>42</sup> The corresponding lifetimes of ANS at 534 nm, 556 nm and 590 nm were 301 ms, 264 ms and 215 ms, respectively, which were consistent with the colour change observed by the naked eye. In addition, corresponding CIE coordinate diagrams were also consistent with the colour of the photos (Fig. 4b), which further proved the time-dependent afterglow characteristics. Therefore, ANS@ $\epsilon$ -PL can be used as an ideal candidate for advanced anti-counterfeiting and encryption.

These interesting results encouraged us to continue to explore the luminous mechanism of RTP. After the guest molecules were doped into  $\epsilon$ -PL, the successful emission of phosphorescence and afterglow was attributed to the rigid environment provided by  $\epsilon$ -PL, which effectively protected the guest phosphor molecules from the quenching of oxygen and water. The large number of amino and amide groups in  $\epsilon$ -PL facilitates the formation of rigid hydrogen-bond networks within the polymer and between the guest molecules. In addition, the guest molecules are heterocyclic polynuclear aromatic compounds containing N, O, and S heteroatoms, which can trigger  $n$ - $\pi$  transitions to produce a large number of triple

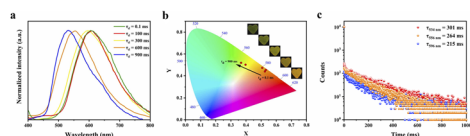


Fig. 4 (a) Delayed emission spectra. (b) CIE coordinate diagrams of ANS@ $\epsilon$ -PL with different times corresponding to delayed emission spectra. The inset photos in (b) show the ANS@ $\epsilon$ -PL afterglows at different times. (c) Time-resolved emission attenuation curves of ANS@ $\epsilon$ -PL films at different wavelengths taken under 365 nm UV light.

excitations.<sup>40,43</sup> Within the relatively rigid environment composed of the  $\epsilon$ -PL matrix, the triplet excitons of heterocyclic chromophores can be effectively stabilized to generate the RTP emission by suppressing non-radiative decay through abundant hydrogen-bond interactions (Fig. 5a). Moreover, the presence of dipole-dipole interactions and electrostatic interactions in the RTP films (ESI Fig. S14<sup>†</sup>) further inhibits non-radiative transition and promotes phosphorescence emission. Specifically, the XRD diffraction peaks of the  $\epsilon$ -PL-based RTP films were rather weak and very wide (Fig. 5b), indicating the amorphous characteristics of these materials, which were conducive to their processing and application. Differential scanning calorimetry (DSC) (Fig. 5c) showed that the RTP materials doped with the guest molecules had good stability,  $T_g$  was in the range of 90–103 °C (ESI Fig. S15<sup>†</sup>), and they were not easy to decompose and deteriorate at room temperature. Thermogravimetric analysis (TGA) (Fig. 5d and e) showed that the decomposition temperature of the  $\epsilon$ -PL films doped with the guest molecules was above 250 °C, which proved that the RTP materials had good thermal stability. Subsequently, to further study the mechanism of RTP, the  $\epsilon$ -PL systems were theoretically calculated based on density functional theory (DFT). In the case of Apyr@ $\epsilon$ -PL, there were four channels ( $\Delta E_{ST} < 0.37$  eV) from singlet  $S_1$  to triplet states to complete the intersystem crossing (ISC), including  $S_1 \rightarrow T_2$ ,  $S_1 \rightarrow T_3$ ,  $S_1 \rightarrow T_4$  and  $S_1 \rightarrow T_5$  (ESI, Table S7<sup>†</sup>). More channels were conducive to the generation of triplet excitons, which led to the emission of phosphorescence. In addition, natural transition orbitals (NTOs) analysis showed that the RTP of Apyr@ $\epsilon$ -PL stemmed from the transitions of  $^3LE$  and  $^1LE$  states (ESI Fig. S20<sup>†</sup>).

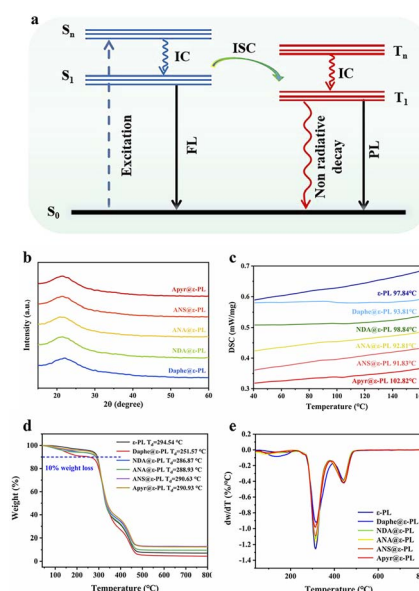


Fig. 5 (a) Jablonski diagram energy level diagram of RTP materials. FL, fluorescence; PL, phosphorescence; ISC, intersystem crossing; and IC, internal conversion. (b) Powder XRD patterns of the five  $\epsilon$ -PL-based RTP films. (c) DSC curves of the  $\epsilon$ -PL-based RTP films. (d) TGA curves of the  $\epsilon$ -PL-based RTP films. (e) DTG curves of the  $\epsilon$ -PL-based RTP films.

To study the humidity response behavior of the  $\epsilon$ -PL-based RTP films, a steam fumigation/heating drying experiment was carried out. Taking NDA as an example, the prepared NDA@ $\epsilon$ -PL still retained its room-temperature phosphorescence and emitted green phosphorescence under the excitation of 365 nm UV light. Then, this dry film was sprayed with water, and the mass of the film was taken as an equivalent. When the mass fraction of added water increased from 0 to 100%, a sharp decline in the intensity and lifetime of the afterglow could be observed (Fig. 6a), and the reciprocal of the afterglow time was positively correlated with the mass fraction of water (Fig. 6c), indicating that the afterglow materials were humidity-responsive. Based on this, the material could be applied in a sensor to realize the rapid detection of water content. In addition, the reversibility and fatigue resistance of the material to water stimulation were also investigated. After repeating the water stimulation/drying cycle four times, the duration and intensity of the phosphorescence emission were not significantly reduced (Fig. 6b). To further explore the mechanism of phosphorescence in response to humidity stimulation, the Fourier transform infrared spectra (FTIR) of  $\epsilon$ -PL-based RTP films were obtained (Fig. 6d–h). After water stimulation, the peak of the material at 3000–3500  $\text{cm}^{-1}$  became wider and stronger, and the peak at 3300  $\text{cm}^{-1}$  was caused by the hydroxyl group in water and amino groups in the  $\epsilon$ -PL chain, and the wider peak indicated the greater water content. The added water destroyed the original rigid hydrogen-bond network and formed a new loose hydrogen-bond network with  $\epsilon$ -PL, resulting in the increase of the non-radiative transition; in addition, it could quench the triplet excitons, making the afterglow weaken or even disappear. When the films were heated to remove water, the original hydrogen-bond network and afterglow were restored.

To further verify the superiority of the  $\epsilon$ -PL matrix, PMMA was selected as a matrix for comparison. First, because PMMA does not contain functional groups such as amino and carboxyl groups, it could be well proved that amino and carboxyl groups in  $\epsilon$ -PL can form abundant hydrogen bonds with the guest molecules.

Second, although PMMA is soluble in dichloromethane and  $\epsilon$ -PL dissolves in water, both RTP materials were obtained after drying to remove the solvent, resulting in no serious effect on the final conclusion. After changing the substrate, the lifetime of the phosphor was found to be significantly reduced by 5 orders of magnitude compared to the lifetime of the  $\epsilon$ -PL matrix (ESI, Fig. S21<sup>†</sup>), proving that the  $\epsilon$ -PL matrix plays an important role in inhibiting non-radiative transition and preventing phosphorescence quenching. In addition to the matrix, the functional groups contained in the guest molecules also play a vital role in the afterglow emissions. This is because these functional groups not only form hydrogen bonds with the matrix to inhibit non-radiative transition, but also the lone pair electrons carried by the heteroatoms in the functional groups to enhance the spin-orbit coupling (SOC). To verify the important role of functional groups, some guest molecules without amino and carboxyl groups were selected for doping. When phenanthrene (phe), naphthalene (Naph), 2-naphthalic acid (NA), 2-naphthalene sulfonic acid (NS) and pyrene (pyr) were doped into  $\epsilon$ -PL, their lifetimes were found to be reduced to the millisecond or even nanosecond level (ESI Fig. S22<sup>†</sup>), which fully proved the important role of these functional groups in the afterglow emissions.

## Applications

Based on the adjustable colour and multiple stimulus response properties of the prepared amorphous  $\epsilon$ -PL-based RTP films, they display great prospects for application in data encryption and anti-counterfeiting. The prepared material can be made into encryption ink in solution state. As shown in Fig. 7a, five letters OURTP, abbreviation for organic ultralong room temperature phosphorescence, were written on the filter paper with five types of  $\epsilon$ -PL suspension with 1% mass fraction using this ink. After drying, they were almost invisible at room temperature, but under the excitation of 365 nm UV light, the blue fluorescence began to appear. When the excitation light source was removed, the letters immediately changed to a bright multi-colour pattern. The RTP materials could also be

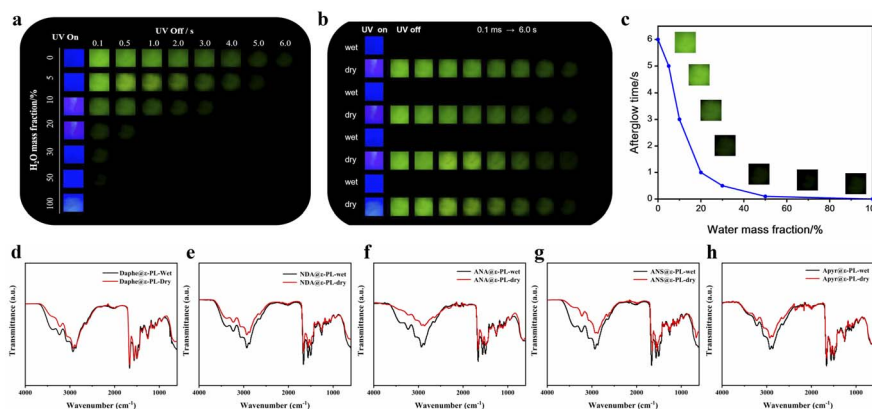


Fig. 6 (a) Schematic diagram of the change in the NDA@ $\epsilon$ -PL afterglow with different water contents taken under 365 nm UV light. (b) Photographs of the steam fumigation/heating drying of NDA@ $\epsilon$ -PL. (c) Line chart of NDA@ $\epsilon$ -PL afterglow time with different water contents. The inset photos in (c) show the afterglows with different water contents. (d–h) FTIR spectra of the  $\epsilon$ -PL-based RTP films under the stimuli of steam fumigation/heating drying.

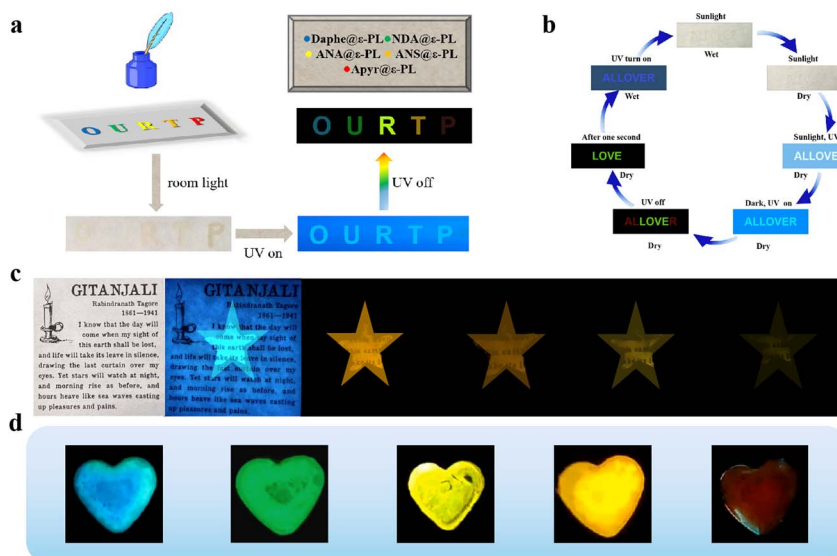


Fig. 7 (a) Demonstration of encryption by combining five different materials. (b) Diagram of multiple encryption composed of ANA@ $\epsilon$ -PL and Apyr@ $\epsilon$ -PL. (c) Photographs of anti-counterfeiting label printed with ANS@ $\epsilon$ -PL material. (d) Schematic of five materials processed into arbitrary shapes.

used for anti-counterfeiting on valuable documents, such as letters. Fig. 7c shows a poem by Tagore, which looked nothing special on the surface, but when irradiated with 365 nm UV light, it would show blue fluorescence, and the afterglow was time-dependent. This provides a simple method for anti-counterfeiting and combatting piracy. Since the phosphorescence lifetime of each material is different, the corresponding afterglow duration was also different; thus, the materials could also provide various coding procedures for data encryption. The characters of ALLOVER were drawn on paper (Fig. 7b), where letters “A”, “L” and “R” were written using a suspension of Apyr@ $\epsilon$ -PL, and the letters of “LOVE” were written using a suspension of ANA@ $\epsilon$ -PL. In sunlight, the letters were faintly visible when wet, while the contents were hidden when dried. When illuminated by 365 nm UV light, the letters showed blue fluorescence, and after removing the excitation light source, the letters appeared in different colours. A second later, “ALR” disappeared, leaving only the characters of “LOVE”, thus creating the effect of multiple encryption. Furthermore, the performance of the materials did not change significantly after repeated water treatment; hence, the materials have good reversibility and can be reused. The identifiable RTP properties and film-forming capabilities enriched the coding range of these flexible organic materials (Fig. 7d). Remarkably, the long-life RTP materials with colour-tunable, excitation-dependent and time-dependent properties provide a very high level of security for protecting significant information.

## Conclusions

In summary, a series of colour-adjustable RTP materials with multiple stimulus responses have been prepared by doping guest phosphor molecules into the  $\epsilon$ -PL matrix. On the one

hand, the heteroatoms in the functional groups such as amino and carboxyl groups promoted spin-orbit coupling and ISC processes. On the other hand, a rigid hydrogen-bond network was formed within  $\epsilon$ -PL and the guest molecules to inhibit non-radiative relaxation, promoted triplet emission, and finally provided RTP with an afterglow duration of up to 15 s under environmental conditions. The RTP emitted by these amorphous materials has significant tunability from blue (464 nm) to red (693 nm), with quantum yields and phosphorescence lifetimes as high as 18.84% and 2504.7 ms, respectively. Interestingly, Daphe@ $\epsilon$ -PL films had Ex-De properties owing to their different emission centers. As the excitation wavelength increased from 254 nm to 365 nm, the emission wavelength redshifted from 461 nm to 530 nm, while ANS@ $\epsilon$ -PL films showed time-dependent afterglows. As the delay time extended, the peak wavelength of its spectrum also presented a blueshift. In addition,  $\epsilon$ -PL-based RTP materials had good reversibility and fatigue resistance to water stimulus, so they can be applied in sensors to achieve rapid detection of water content. Moreover, RTP characteristics, excellent water solubility and film-forming ability give these materials broad application prospects, such as in multiple encryption and anti-counterfeiting. These findings will further promote the development of polymer-based phosphor materials.

## Data availability

The data supporting this article have been included in ESI.†

## Author contributions

Jiaying Cui: conceptualization, formal analysis, investigation, validation, visualization, writing – original draft, and writing –

review & editing. Syed Husnain Ali: formal analysis and software. Zhuoyao Shen: supervision, methodology, and formal analysis. Wensheng Xu: software, data curation, and formal analysis. Jiayi Liu: data curation and project administration. Pengxiang Li: data curation and formal analysis. Yang Li: resources, supervision, data curation, project administration and writing – review & editing. Ligong Chen: methodology, supervision, project administration, and writing – review & editing. Bowei Wang: supervision, project administration and writing – review & editing.

## Conflicts of interest

There are no conflicts to declare.

## Acknowledgements

The authors thank Danyu Gu from Instrumentation and Service Center for Molecular Sciences at Westlake University for the assistance in measurement.

## Notes and references

- 1 S. Xu, R. Chen, C. Zheng and W. Huang, Excited State Modulation for Organic Afterglow: Materials and Applications, *Adv. Mater.*, 2016, **28**, 9920–9940.
- 2 Y. Zhang, S. Zhang, G. Liu, Q. Sun, S. Xue and W. Yang, Rational molecular and doping strategies to obtain organic polymers with ultralong RTP, *Chem. Sci.*, 2023, **14**, 5177–5181.
- 3 X. Dou, T. Zhu, Z. Wang, W. Sun, Y. Lai, K. Sui, Y. Tan, Y. Zhang and W. Z. Yuan, Color-Tunable, Excitation-Dependent, and Time-Dependent Afterglows from Pure Organic Amorphous Polymers, *Adv. Mater.*, 2020, **32**, e2004768.
- 4 Z. He, H. Gao, S. Zhang, S. Zheng, Y. Wang, Z. Zhao, D. Ding, B. Yang, Y. Zhang and W. Z. Yuan, Achieving Persistent, Efficient, and Robust Room-Temperature Phosphorescence from Pure Organics for Versatile Applications, *Adv. Mater.*, 2019, **31**, e1807222.
- 5 H. Ma, Q. Peng, Z. An, W. Huang and Z. Shuai, Efficient and Long-Lived Room-Temperature Organic Phosphorescence: Theoretical Descriptors for Molecular Designs, *J. Am. Chem. Soc.*, 2019, **141**, 1010–1015.
- 6 H. Qiu, W. Wang, H. Cheng, Y. Lu, M. Li, H. Chen, X. Fang, C. Jiang and Y. Zheng, Triple optically modulated and enzymatically responsive organic afterglow materials for dynamic anti-counterfeiting, *Mater. Chem. Front.*, 2022, **6**, 1824–1834.
- 7 T. Wang, X. Su, X. Zhang, X. Nie, L. Huang, X. Zhang, X. Sun, Y. Luo and G. Zhang, Aggregation-Induced Dual-Phosphorescence from Organic Molecules for Nondoped Light-Emitting Diodes, *Adv. Mater.*, 2019, **31**, e1904273.
- 8 S. Zheng, T. Zhu, Y. Wang, T. Yang and W. Z. Yuan, Accessing Tunable Afterglows from Highly Twisted Nonaromatic Organic AIEgens via Effective Through-Space Conjugation, *Angew Chem. Int. Ed. Engl.*, 2020, **59**, 10018–10022.
- 9 W. Zhao, Z. He and B. Z. Tang, Room-temperature phosphorescence from organic aggregates, *Nat. Rev. Mater.*, 2020, **5**, 869–885.
- 10 L. Gu, H. Shi, L. Bian, M. Gu, K. Ling, X. Wang, H. Ma, S. Cai, W. Ning, L. Fu, H. Wang, S. Wang, Y. Gao, W. Yao, F. Huo, Y. Tao, Z. An, X. Liu and W. Huang, Colour-tunable ultralong organic phosphorescence of a single-component molecular crystal, *Nat. Photonics*, 2019, **13**, 406–411.
- 11 X. N. Li, M. Yang, X. L. Chen, J. H. Jia, W. W. Zhao, X. Y. Wu, S. S. Wang, L. Meng and C. Z. Lu, Synergistic Intra- and Intermolecular Noncovalent Interactions for Ultralong Organic Phosphorescence, *Small*, 2019, **15**, 1903270.
- 12 X. K. Ma and Y. Liu, Supramolecular Purely Organic Room-Temperature Phosphorescence, *Acc. Chem. Res.*, 2021, **54**, 3403–3414.
- 13 Z. Y. Zhang, W. W. Xu, W. S. Xu, J. Niu, X. H. Sun and Y. Liu, A Synergistic Enhancement Strategy for Realizing Ultralong and Efficient Room-Temperature Phosphorescence, *Angew Chem. Int. Ed. Engl.*, 2020, **59**, 18748–18754.
- 14 M. Hayduk, S. Riebe and J. Voskuhl, Phosphorescence Through Hindered Motion of Pure Organic Emitters, *Chemistry*, 2018, **24**, 12221–12230.
- 15 J. X. Wang, Y. G. Fang, C. X. Li, L. Y. Niu, W. H. Fang, G. Cui and Q. Z. Yang, Time-Dependent Afterglow Color in a Single-Component Organic Molecular Crystal, *Angew Chem. Int. Ed. Engl.*, 2020, **59**, 10032–10036.
- 16 L. Sun, W. Zhu, F. Yang, B. Li, X. Ren, X. Zhang and W. Hu, Molecular cocrystals: design, charge-transfer and optoelectronic functionality, *Phys. Chem. Chem. Phys.*, 2018, **20**, 6009–6023.
- 17 B. Zhou and D. Yan, Hydrogen-Bonded Two-Component Ionic Crystals Showing Enhanced Long-Lived Room-Temperature Phosphorescence via TADF-Assisted Förster Resonance Energy Transfer, *Adv. Funct. Mater.*, 2019, **29**, 1807599.
- 18 Y. Deng, D. Zhao, X. Chen, F. Wang, H. Song and D. Shen, Long lifetime pure organic phosphorescence based on water soluble carbon dots, *Chem. Commun.*, 2013, **49**, 5751–5753.
- 19 Y. Sun, S. Liu, L. Sun, S. Wu, G. Hu, X. Pang, A. T. Smith, C. Hu, S. Zeng, W. Wang, Y. Liu and M. Zheng, Ultralong lifetime and efficient room temperature phosphorescent carbon dots through multi-confinement structure design, *Nat. Commun.*, 2020, **11**, 5591.
- 20 K. Wang, L. Qu and C. Yang, Long-Lived Dynamic Room Temperature Phosphorescence from Carbon Dots Based Materials, *Small*, 2023, **19**, 2206429.
- 21 W. H. Lv, Q. Cao, S. Y. Song, Y. C. Liang, R. Zhou, K. K. Liu and C. X. Shan, Enhanced Phosphorescence of Carbon Nanodots via Double Confinement for 3D Artworks with Long Emission Lifetimes, *Small*, 2023, **19**, 2302504.
- 22 H. Shi, Z. An, P.-Z. Li, J. Yin, G. Xing, T. He, H. Chen, J. Wang, H. Sun, W. Huang and Y. Zhao, Enhancing Organic Phosphorescence by Manipulating Heavy-Atom Interaction, *Cryst. Growth Des.*, 2016, **16**, 808–813.
- 23 J. Yuan, S. Wang, Y. Ji, R. Chen, Q. Zhu, Y. Wang, C. Zheng, Y. Tao, Q. Fan and W. Huang, Invoking ultralong room

- temperature phosphorescence of purely organic compounds through H-aggregation engineering, *Mater. Horiz.*, 2019, **6**, 1259–1264.
- 24 J. Guo, C. Yang and Y. Zhao, Long-Lived Organic Room-Temperature Phosphorescence from Amorphous Polymer Systems, *Acc. Chem. Res.*, 2022, **55**, 1160–1170.
- 25 Z. Lin, R. Kabe, N. Nishimura, K. Jinnai and C. Adachi, Organic Long-Persistent Luminescence from a Flexible and Transparent Doped Polymer, *Adv. Mater.*, 2018, **30**, e1803713.
- 26 X. Zhang, Y. Cheng, J. You, J. Zhang, C. Yin and J. Zhang, Ultralong phosphorescence cellulose with excellent antibacterial, water-resistant and ease-to-process performance, *Nat. Commun.*, 2022, **13**, 1117.
- 27 S. Cai, H. Shi, J. Li, L. Gu, Y. Ni, Z. Cheng, S. Wang, W. W. Xiong, L. Li, Z. An and W. Huang, Visible-Light-Excited Ultralong Organic Phosphorescence by Manipulating Intermolecular Interactions, *Adv. Mater.*, 2017, **29**, 1701244.
- 28 N. Gan, H. Shi, Z. An and W. Huang, Recent Advances in Polymer-Based Metal-Free Room-Temperature Phosphorescent Materials, *Adv. Funct. Mater.*, 2018, **28**, 1802657.
- 29 D. Lee, O. Bolton, B. C. Kim, J. H. Youk, S. Takayama and J. Kim, Room temperature phosphorescence of metal-free organic materials in amorphous polymer matrices, *J. Am. Chem. Soc.*, 2013, **135**, 6325–6329.
- 30 T. Sakurai, N. Orito, S. Nagano, K. Kato, M. Takata and S. Seki, Electron-transporting foldable alternating copolymers of perylenediimide and flexible macromolecular chains, *Mater. Chem. Front.*, 2018, **2**, 718–729.
- 31 B. Wu, N. Guo, X. Xu, Y. Xing, K. Shi, W. Fang and G. Wang, Ultralong and High-Efficiency Room Temperature Phosphorescence of Organic-Phosphors-Doped Polymer Films Enhanced by 3D Network, *Adv. Opt. Mater.*, 2020, **8**, 2001192.
- 32 T. Weng, G. Baryshnikov, C. Deng, X. Li, B. Wu, H. Wu, H. Ågren, Q. Zou, T. Zeng and L. Zhu, A Fluorescence-Phosphorescence-Phosphorescence Triple-Channel Emission Strategy for Full-Color Luminescence, *Small*, 2020, **16**, 1906475.
- 33 Y. Lei, W. Dai, J. Guan, S. Guo, F. Ren, Y. Zhou, J. Shi, B. Tong, Z. Cai, J. Zheng and Y. Dong, Wide-Range Color-Tunable Organic Phosphorescence Materials for Printable and Writable Security Inks, *Angew Chem. Int. Ed. Engl.*, 2020, **59**, 16054–16060.
- 34 Z. Qu, Y. Guo, J. Zhang and Z. Zhou, Mesomerism induced temperature-dependent multicomponent phosphorescence emissions in ClBDBT, *Chem. Sci.*, 2023, **14**, 10096–10102.
- 35 D. Malpicci, A. Forni, C. Botta, C. Giannini, E. Lucenti, D. Marinotto, D. Maver, L. Carlucci and E. Cariati, Stimuli Responsive Features of Organic RTP Materials: An Intriguing Carbazole-Cyclic Triimidazole Derivative, *Chemistry*, 2023, e202300930, DOI: [10.1002/chem.202300930](https://doi.org/10.1002/chem.202300930).
- 36 Y. Su, Y. Zhang, Z. Wang, W. Gao, P. Jia, D. Zhang, C. Yang, Y. Li and Y. Zhao, Excitation-Dependent Long-Life Luminescent Polymeric Systems under Ambient Conditions, *Angew Chem. Int. Ed. Engl.*, 2020, **59**, 9967–9971.
- 37 L. Bian, H. Shi, X. Wang, K. Ling, H. Ma, M. Li, Z. Cheng, C. Ma, S. Cai, Q. Wu, N. Gan, X. Xu, Z. An and W. Huang, Simultaneously Enhancing Efficiency and Lifetime of Ultralong Organic Phosphorescence Materials by Molecular Self-Assembly, *J. Am. Chem. Soc.*, 2018, **140**, 10734–10739.
- 38 L. Gu, H. Shi, C. Miao, Q. Wu, Z. Cheng, S. Cai, M. Gu, C. Ma, W. Yao, Y. Gao, Z. An and W. Huang, Prolonging the lifetime of ultralong organic phosphorescence through dihydrogen bonding, *J. Mater. Chem. C*, 2018, **6**, 226–233.
- 39 Z. Xie, X. Zhang, H. Wang, C. Huang, H. Sun, M. Dong, L. Ji, Z. An, T. Yu and W. Huang, Wide-range lifetime-tunable and responsive ultralong organic phosphorescent multi-host/guest system, *Nat. Commun.*, 2021, **12**, 3522.
- 40 H. Wu, W. Chi, Z. Chen, G. Liu, L. Gu, A. K. Bindra, G. Yang, X. Liu and Y. Zhao, Achieving Amorphous Ultralong Room Temperature Phosphorescence by Coassembling Planar Small Organic Molecules with Polyvinyl Alcohol, *Adv. Funct. Mater.*, 2019, **29**, 1807243.
- 41 Y. Su, Y. Zhang, Z. Wang, W. Gao, P. Jia, D. Zhang, C. Yang, Y. Li and Y. Zhao, Excitation-Dependent Long-Life Luminescent Polymeric Systems under Ambient Conditions, *Angew. Chem.*, 2019, **132**, 10053–10057.
- 42 Z. Wang, A. Li, Z. Zhao, T. Zhu, Q. Zhang, Y. Zhang, Y. Tan and W. Z. Yuan, Accessing Excitation- and Time-Responsive Afterglows from Aqueous Processable Amorphous Polymer Films through Doping and Energy Transfer, *Adv. Mater.*, 2022, **34**, 2202182.
- 43 Y. Zhang, Y. Su, H. Wu, Z. Wang, C. Wang, Y. Zheng, X. Zheng, L. Gao, Q. Zhou, Y. Yang, X. Chen, C. Yang and Y. Zhao, Large-Area, Flexible, Transparent, and Long-Lived Polymer-Based Phosphorescence Films, *J. Am. Chem. Soc.*, 2021, **143**, 13675–13685.